Integrin-mediated axoglial interactions initiate myelination in the central nervous system

Joana Câmara,[1] Zhen Wang,[1] Cristina Nunes-Fonseca,[1,5] Hana C. Friedman,[2] Matthew Grove,[3] Diane L. Sherman,[3] Noboru H. Komiyama,[4] Seth G. Grant,[3,4] Peter J. Brophy,[3] Alan Peterson,[2] and Charles ffrench-Constant[1,5]

[1]Department of Pathology, University of Cambridge, Cambridge CB2 1QP, England, UK
[2]Laboratory of Developmental Biology, Royal Victoria Hospital H-5, McGill University Health Centre, Montreal, Quebec H3A 1A1, Canada
[3]Centre for Neuroscience Research, University of Edinburgh, Edinburgh EH8 9JZ, Scotland, UK
[4]Genes to Cognition Programme, Wellcome Trust Sanger Institute, Cambridge CB10 1SA, England, UK
[5]MRC Centre for Regenerative Medicine, Centre for MS Research, Queen's Medical Research Institute, Edinburgh EH16 4TJ, Scotland, UK

All but the smallest-diameter axons in the central nervous system are myelinated, but the signals that initiate myelination are unknown. Our prior work has shown that integrin signaling forms part of the cell–cell interactions that ensure only those oligodendrocytes contacting axons survive. Here, therefore, we have asked whether integrins regulate the interactions that lead to myelination. Using homologous recombination to insert a single-copy transgene into the hypoxanthine phosphoribosyl transferase (hprt) locus, we find that mice expressing a dominant-negative $\beta 1$ integrin in myelinating oligodendrocytes require a larger axon diameter to initiate timely myelination. Mice with a conditional deletion of focal adhesion kinase (a signaling molecule activated by integrins) exhibit a similar phenotype. Conversely, transgenic mice expressing dominant-negative $\beta 3$ integrin in oligodendrocytes display no myelination abnormalities. We conclude that $\beta 1$ integrin plays a key role in the axoglial interactions that sense axon size and initiate myelination, such that loss of integrin signaling leads to a delay in myelination of small-diameter axons.

Introduction

Myelination represents a spectacular cell–cell interaction in which axons are ensheathed by multiple layers of membrane from specialized glia—oligodendrocytes in the central nervous system (CNS) and Schwann cells in the peripheral nervous system (PNS). The threshold axon diameter for myelination is a regulated process, with a minimum axon diameter for myelination of 1 µm in the PNS and of 0.2 µm in the CNS (Waxman and Bennett, 1972; Voyvodic, 1989). Moreover, the number of wraps is precisely related to the axon diameter such that the ratio of the diameter of the axon to that of the entire myelinated unit—the g-ratio—is constant (Friede, 1972). This points to the existence of signals on the axon surface that both initiate the myelination process and then determine exactly how many times the myelinating process wraps around the axon before the extrusion of cytoplasm (a process termed compaction) and the formation of the mature multilamellar sheath. In the PNS, a necessary and sufficient signal is type III neuregulin-1 (Nrg1), increased expression of which on the axon results in a thicker myelin sheath, whereas reduced axonal expression results in thinner myelin (Michailov et al., 2004; Taveggia et al., 2005). The overexpression of Nrg1 also causes the myelination of axons whose size is below the normal threshold (Taveggia et al., 2005), showing that Nrg1 is a signal that initiates myelination in addition to its role in regulating wrapping. In the CNS, however, the role and identity of any such initiation signals remains unknown, with the contribution of neuregulins at this and later stages of myelination being unclear. Although type III Nrg1$^{+/-}$ mice show reduced myelin sheath thickness in the corpus callosum (Taveggia et al., 2008), normal myelination in mice where the Nrg1 gene has been excised in the CNS (Brinkmann et al., 2008) shows that other signals must contribute to the precise relationship between axon and oligodendrocyte.

Cell adhesion molecules represent excellent candidates for these additional signals regulating myelination (Laursen and ffrench-Constant, 2007). One of these is $\alpha 6 \beta 1$ integrin, a receptor expressed on oligodendrocytes for laminins expressed in

Correspondence to Charles ffrench-Constant: cffc@ed.ac.uk

Abbreviations used in this paper: CNS, central nervous system; DRG, dorsal root ganglion; ES, embryonic stem; hprt, hypoxanthine phosphoribosyl transferase; MBP, myelin basic protein; PNS, peripheral nervous system.

THE JOURNAL OF CELL BIOLOGY

axon tracts at the time of myelination that promotes oligoden-drocyte survival by amplification of growth factor signaling (Colognato et al., 2002). This provides a mechanism for the target-dependent survival of oligodendrocytes, with those that fail to establish normal contact with axons during development undergoing programmed cell death. The importance of integrins in oligodendrocyte biology is further underscored by the finding that integrin-mediated signaling pathways are strongly represented in a genome-wide analysis of expression in differentiating oligodendrocytes (Cahoy et al., 2008). Here, therefore, we have asked whether integrins play a role in the regulation of myelination, either by contributing to the signals that initiate myelination or by regulating the thickness of the resulting myelin sheath.

Prior studies on the role of β1 integrin in CNS myelination in vivo have been contradictory. Constitutive disruption of the β1 integrin gene resulted in early lethality (Fassler and Meyer, 1995; Stephens et al., 1995), requiring the use of conditional ablation or dominant-negative strategies to examine function. Lee et al. (2006) reported that mice expressing a β1 integrin lacking the C-terminal cytoplasmic tail (β1ΔC) in oligodendrocytes displayed region-specific hypomyelination in optic nerve and spinal cord and no myelination abnormalities in the corpus callosum. In contrast, conditional inactivation of the β1 integrin gene in premyelinating oligodendrocytes showed that β1 integrin is not required for CNS axon ensheathment, myelination, or remyelination (Benninger et al., 2006). Nonetheless, the contribution made by integrin signaling to oligodendrocyte survival, evidenced by our earlier studies on the α6 knockout CNS, was confirmed by a transient reduction in oligodendrocyte numbers in the developing cerebellum (Benninger et al., 2006). However, it is possible that both these studies fail to reveal the specific function of β1 integrin in myelinating oligodendrocytes. In the knockout study, gene deletion occurs early, at the premyelinating stage of oligodendrocyte development, thus potentially enabling compensation by other integrins to occur by the stage of myelination. The ability of different integrin β subunits to compensate for one another has been previously shown in *Drosophila* embryogenesis (Martin-Bermudo et al., 1999). In the dominant-negative study, the construct used by Lee et al. (2006) contained a normal integrin extracellular domain that will bind laminin and compete with any other laminin receptors for available ligand in the myelinating tract. Here, therefore, we have used the reverse strategy—expression in oligodendrocytes of a well-characterized dominant-negative β1 integrin subunit containing only the intracellular domain that will not bind ligand and would thus be predicted to be more specific in targeting β1 integrin signaling (LaFlamme et al., 1994; Relvas et al., 2001). Furthermore, we have minimized the time available for compensatory mechanisms to develop by expressing the dominant-negative subunit only at the myelinating stage in oligodendrocytes using the myelin basic protein (MBP) promoter (Farhadi et al., 2003).

Results

Generation of dominant-negative β1 integrin transgenic mice (dnβ1)

To examine the role of β1 integrin signaling in myelination in vivo, without perturbing the earlier stages of oligodendrocyte precursor migration and proliferation, we generated transgenic mice expressing a dominant-negative chimeric β1 integrin (dnβ1) under the control of the 9.5-Kb MBP promoter. This promoter drives specific expression in myelinating oligodendrocytes within the CNS (Farhadi et al., 2003), as we confirmed in lacZ reporter mice that showed expression of β-galactosidase only at the time of myelination in different white matter tracts (Fig. S1). The dominant-negative construct used contains the β1 intracellular domain and the extracellular and transmembrane domains were replaced by the nonsignaling α-subunit of the human interleukin-2 receptor (IL2Rα). This chimeric integrin has been shown to function in a dominant-negative manner in vitro (LaFlamme et al., 1994) and when expressed in oligodendrocyte precursors transplanted into demyelinated lesions (Relvas et al., 2001).

To overcome the usual limitations of random and multiple-copy insertion in standard transgenesis, we used the hypoxanthine phosphoribosyl transferase (hprt) targeting system (Farhadi et al., 2003) for the generation of the genetically modified embryonic stem (ES) cells expressing the dnβ1 integrin (Fig. 1 a). This technology uses homologous recombination to target a single copy of the desired transgene (in this case the dnβ1 integrin) driven by a specific promoter (in this case the MBP promoter) into the hprt locus on the X-chromosome. The ES cell line used lacks a complete hprt gene and the targeting vector "rescues" the hprt gene by replacing the lost sequences in addition to inserting the desired transgene and its promoter. As a result, ES cells with the correct insertion can easily be selected by virtue of their expression of hprt and the subsequent ability to grow in HAT medium. This process was extremely efficient, with 12 out of 12 clones selected having the correct insertion, as evidenced by PCR analysis performed as described in the Materials and methods (Fig. 1 b). We then generated transgenic mice from one of these ES cell lines to establish a dnβ1 transgenic line. These mice had no overt phenotype, and in particular showed no evidence of locomotor defects.

A second major advantage of using this technology is that single-copy insertion of the transgene into the same place in each line eliminates position and copy number effects, and makes comparison of multiple transgenic lines unnecessary. This has been confirmed by experiments where different mouse lines derived using this strategy from independently targeted ES cell clones expressing the same bcl-2 transgene exhibited comparable levels of expression (Bronson et al., 1996) and by our own previous studies showing that pairs of transgenic lines expressing different MBP regulatory sequences show similar levels of β-galactosidase expression within each pair (Farhadi et al., 2003). Hemizygous and wild-type littermate males of the single line were therefore used as mutant and control mice, respectively, throughout this study (Fig. 1 c).

Dnβ1 mice express the dominant-negative β1 integrin in white matter tracts

Expression of the dnβ1 integrin in the mutant was initially confirmed by RT-PCR. Primers hybridizing to the human IL2Rα gene, only present in the inserted dominant-negative construct, showed specific amplification in mutant mice (Fig. 2 a). To visualize the expression of the dnβ1 integrin protein in the myelinating tracts,
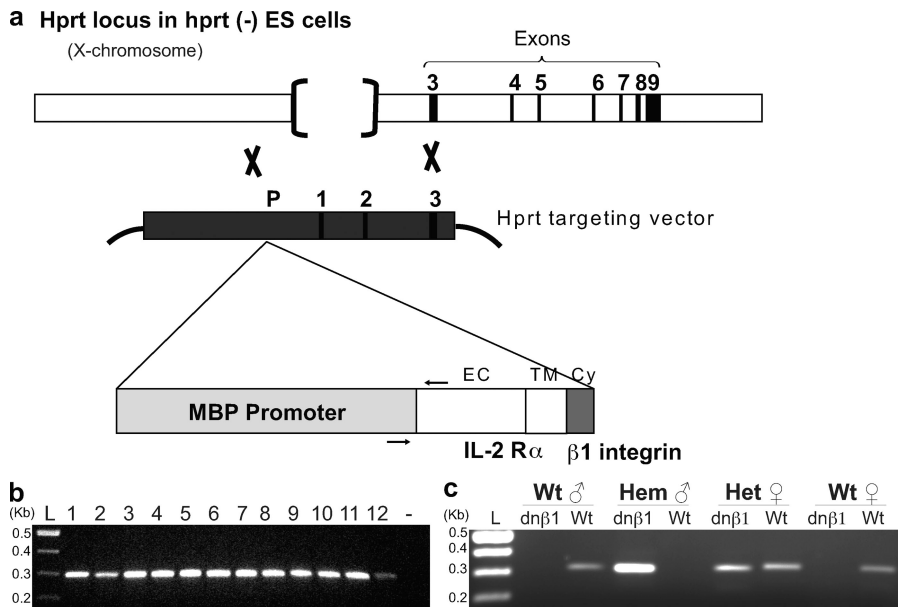
a **Hprt locus in hprt (-) ES cells**
(X-chromosome)

Exons

3   4 5   6 7 89

P 1 2 3   Hprt targeting vector

MBP Promoter   EC   TM Cy

IL-2 Rα   β1 integrin

b
(Kb) L 1 2 3 4 5 6 7 8 9 10 11 12 -
0.5
0.4
0.3
0.2

c
(Kb)   **Wt ♂**   **Hem ♂**   **Het ♀**   **Wt ♀**
L   dnβ1 Wt   dnβ1 Wt   dnβ1 Wt   dnβ1 Wt
0.5
0.4
0.3
0.2

Figure 1. **Generation of dominant-negative β1 integrin transgenic mice (dnβ1).** (a) The hprt targeting system used in our study: the dnβ1 transgene (comprising the IL2Rα extracellular and transmembrane domains and the β1 integrin cytoplasmic domain) and the MBP promoter were inserted by homologous recombination in single copy into the disrupted hprt locus on the X-chromosome of the hprt (−) ES cell line. The targeting vector contains the missing hprt sequences and thus restores hprt functionality and enables subsequent growth of the ES cells in HAT medium. (b) Transfected hprt (−) ES cells bearing a functional hprt gene (after successful recombination) were selected for HAT medium and screened by PCR using the primers represented as arrows in panel a. A band of 290 bp indicates the presence of the dnβ1 transgene. Twelve out of the twelve HAT⁺ clones correctly recombined. (c) Genotyping of transgenic mice was performed by PCR for wild-type (Wt) and dnβ1 transgenic alleles (dnβ1). Genotype of the four animals shown: Wt, wild-type; Hem, hemizygous male; Het, heterozygous. Panel a was adapted from Bronson et al. (1996).

we used immunofluorescence labeling with an anti–human IL2Rα antibody on transverse sections of optic nerve, sagittal sections of cerebellum, and coronal sections of corpus callosum in wild-type and mutant mice (Fig. 2 b). The dnβ1 integrin was expressed in white matter tracts within these regions in mutant mice, whereas no expression was detected in the wild-type animals. These results confirm that the dnβ1 integrin is expressed in transgenic mice at the RNA and protein level in the predicted pattern within myelinating tracts.

Next, we tested if this expression was specific to the nervous system. We analyzed RNA from several tissues of the dnβ1 mice by RT-PCR (Fig. 2 c). Transgene expression was found to be restricted to cortex, cerebellum, brainstem, spinal cord, optic nerve, and sciatic nerve and absent from other tissues such as heart, liver, lungs, kidney, muscle, testis, spleen, and stomach. This confirms that, as we would predict from the known expression pattern of the MBP, the dnβ1 expression is restricted to the nervous system.

Integrin signaling is inhibited in the dnβ1 mice

To confirm the efficacy of our strategy, we asked to what extent the dnβ1 construct expressed in the transgenic mice inhibited the endogenous β1 integrin. First, we compared the expression levels of the endogenous and the transgenic β1 integrin. In vitro studies have demonstrated that approximately equal expression levels of the IL2R-integrin chimera to the endogenous integrin are sufficient to inhibit integrin-mediated cell spreading and migration, confirming that this level of transgene expression exerts a dominant-negative effect (LaFlamme et al., 1994). We therefore designed a semi-quantitative RT-PCR analysis using two distinct sets of primers, one specific for the endogenous β1 integrin and another for the dnβ1 integrin, taking advantage of the differences in their extracellular domains (Fig. 3 a). To examine whether the levels of β1 integrin inhibition might vary in the different areas of the nervous system, we performed

this RT-PCR analysis on several areas of the nervous system. We showed that in all CNS white matter tracts the dnβ1 integrin expression levels were equal to or greater than the levels of the mRNA for the endogenous integrin, with significantly higher levels seen in optic nerve (Fig. 3 b). The same expression pattern was observed in four pairs of mice analyzed, with the mean levels of the dnβ1 mRNA relative to the wild-type β1 mRNA being 2.22 ± 0.37 in optic nerve (P = 0.033), 1.6 ± 0.37 in spinal cord, and 1.22 ± 0.17 in cerebellum, as compared with 0.92 ± 0.10 in cortex.

Second, to show directly that the dominant-negative strategy we used inhibits downstream signaling, as predicted from these expression studies, we examined activation of FAK by tyrosine phosphorylation. Activation of FAK via autophosphorylation, on tyrosine 397, occurs after integrin binding to ECM ligands (Schaller et al., 1994). We showed, by Western blot analysis for P-FAK (Y397), that β1 integrin signaling was significantly reduced ($45 \pm 9.3\%$, P = 0.018, $n = 3$ pairs of animals) in the optic nerve of P18 dnβ1 mice, as compared with wild-type mice of the same age (Fig. 3 c). Similar changes were seen in spinal cord, but these did not reach statistical significance.

The relationship between axon diameter and myelin thickness is normal in dnβ1 mice

To examine myelination in the dnβ1 mice, we first compared white matter tracts in several CNS regions of wild-type and dnβ1 mice by immunohistochemistry using an anti-MBP antibody. We observed no differences in these studies, with the white matter tracts visualized in sections of corpus callosum and optic nerve showing identical thickness and labeling intensity (Fig. S2).

To assess myelination in more detail, we performed an ultrastructural electron microscopy (EM) analysis on optic nerve, spinal cord, and cerebellum at P28, an age when myelination is largely complete (Fig. 4). We found that the relationship between axon diameter and myelin thickness (g-ratio) was not significantly different between dnβ1 mutants and their wild-type
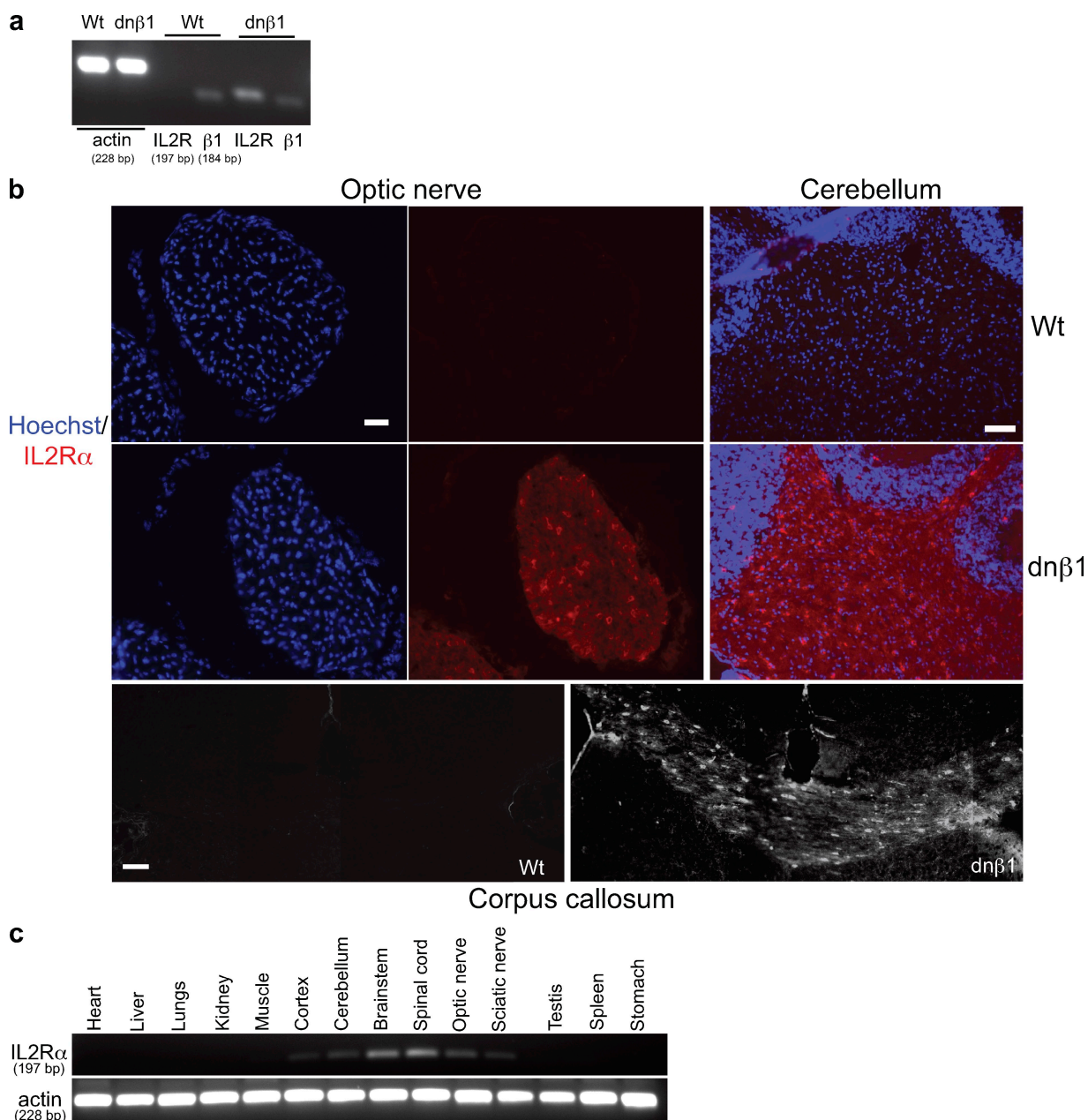
Figure 2. **Dnβ1 mice express the dominant-negative β1 integrin in white matter tracts.** (a) RT-PCR analysis from cortex of 3-mo-old wild-type (Wt) and transgenic mice (dnβ1) reveals RNA expression of β1 integrin in both Wt and transgenic mice but dnβ1 integrin (IL2Rα) only in the mutant. (b) Anti–human IL2Rα immunolabeling of optic nerve transverse sections (bar: 33 µm), cerebellar sagittal sections (bar: 33 µm), and corpus callosum coronal sections (bar: 66 µm) from P18 wild-type and dnβ1 mice shows that the dominant-negative integrin protein is expressed in the myelinating tracts of mutant mice. (c) Dnβ1 expression is nervous system specific as confirmed by an RT-PCR analysis on various tissues from P22 mutant mice. IL2Rα primers were used for detection of the dnβ1 expression (top). Actin primers were used as control (bottom).

counterparts in P28 optic nerve, cerebellum, and spinal cord, with average g-ratios for control and mutant optic nerves of 0.79 ± 0.013 and 0.77 ± 0.020 (P = 0.57); for control and mutant cerebella of 0.80 ± 0.014 and 0.82 ± 0.019 (P = 0.43); for control and mutant spinal cords of 0.80 ± 0.001 and 0.79 ± 0.004 (P = 0.36), respectively. Additionally, no evidence of a higher frequency of dysmyelinated axons in mutant optic nerve, corpus callosum, or spinal cord was observed. We conclude that, for myelinated axons, the myelin morphology and the ratio of myelin thickness/axon diameter in the dnβ1 mutants are the same as in wild-type mice at P28.

The axon diameter required to initiate myelination is increased in the dnβ1 mice

We reasoned that an analysis of development might reveal transient abnormalities of myelination not seen in the fully developed myelinated tracts. We therefore examined optic nerve at P17, a time at which myelination is not yet complete. As in the later stages, no significant differences in the thickness of those myelin sheaths that had formed and appeared fully compacted by this age were detected in the optic nerve (P = 0.65), with average g-ratios for control and mutant mice of 0.79 ± 0.007 and 0.80 ± 0.016, respectively (Fig. 5, a and b). Interestingly, however, we noted at

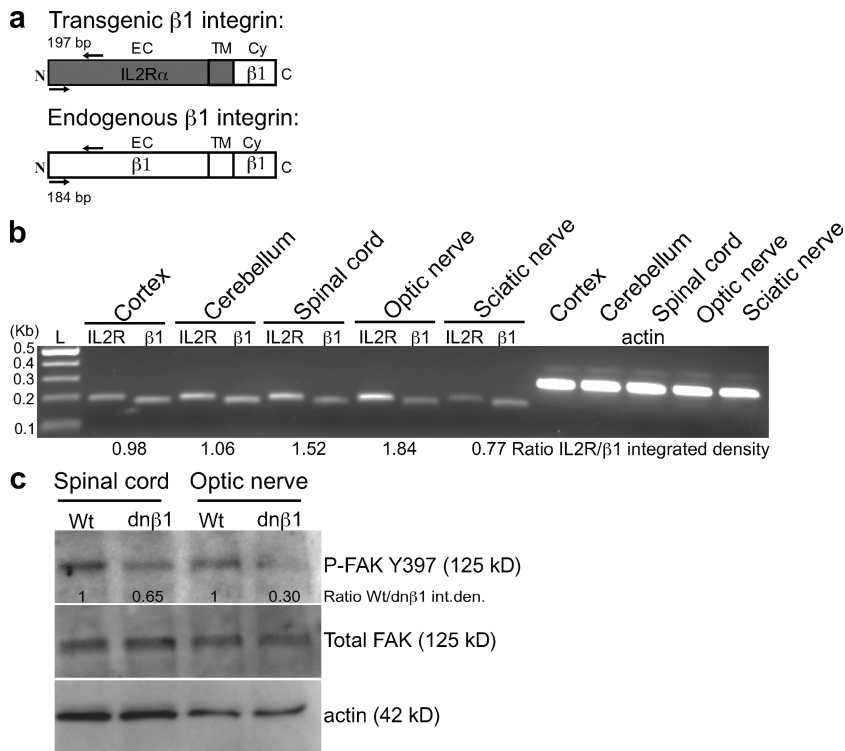**a** Transgenic β1 integrin:

b

c Spinal cord   Optic nerve

Figure 3. **Integrin signaling is inhibited in the dnβ1 mice.** (a) Design of a semi-quantitative RT-PCR using two distinct sets of primers (represented as arrows) binding the extracellular domains of the endogenous (β1) and the transgenic (IL2R) β1 integrins to evaluate their relative expression levels. (b) The dnβ1 integrin (IL2R) is expressed at equal or greater levels than those for the endogenous β1 integrin (β1) in all areas of the CNS, with the highest levels present in spinal cord and optic nerve. A single experiment is shown; quantification of four sets of experiments is presented in the text. (c) Western blot analysis for P-FAK (Y397) shows that integrin downstream signaling is reduced in spinal cord and optic nerve in mutant mice (dnβ1) as compared with the levels seen in wild-type mice (Wt). Antibodies against FAK and actin were used as controls. A single experiment is shown, with quantitative results from three sets of experiments presented in the text.

this age that wild-type oligodendrocytes were myelinating smaller axons to a larger extent than their dnβ1 counterparts. This became apparent in the g-ratio analysis by a reduced population of myelinated axons with small diameters in dnβ1 optic nerves as compared with wild-type nerves (Fig. 5 c). These very small axons must therefore have been unmyelinated in the dnβ1 nerve. We therefore hypothesized that oligodendrocytes with inhibited β1 integrin signaling would require a higher axon diameter to initiate myelination. To address this question, we compared the relationship between axon diameter and the percentage of axons myelinated for wild-type and dnβ1 mice. We measured the axon diameter of more than 400 axons from at least three random nonoverlapping photos and scored them as myelinated or unmyelinated. The axon diameters were then subdivided into 0.1-μm intervals and plotted against the percentage of axons that were myelinated within each interval (Fig. 5 d). As some variability was noted between litters, littermate controls were examined in each case. The percentage of myelinated axons across all axon diameter intervals for the dnβ1 mutant optic nerves (62.08 ± 10.55%, n = 2,494 from 3 animals) was lower (P = 0.023) than for their wild-type littermates (66.30 ± 10.09%, n = 2,506 from 3 animals). This phenotype was most evident in small axons of ≤0.6 μm diameter (P = 0.0085), whereas a similar percentage of myelination was seen in larger axons of >0.6 μm of diameter. In particular, mutant axons of a diameter within the 0.3–0.4-μm range showed the most significant reduction in myelination as compared with wild-type controls (P = 0.023). These results therefore show that the threshold diameter required to initiate myelination is increased in the dnβ1 optic nerve.

To confirm that this effect was transient and only seen during myelinating stages of development, we next repeated the analysis on the older P28 optic nerves. Here no difference was seen between wild-type and dnβ1 littermate animals (Fig. S3),

showing that the effect of loss of integrin signaling is only on the initiation of myelination and results in a delay, rather than in a long-lasting perturbation, in the formation of normal myelin sheaths. This correction resulted from restoration of the ability of the mutant oligodendrocytes to myelinate smaller-diameter axons with age, rather than an overall increase in axon diameter, as evidenced by the higher percentage of axons with a diameter less than 0.5 μm that are myelinated at P28. Thus, at P17 the percentage of axons myelinated of diameters 0.2–0.3, 0.3–0.4 and 0.4–0.5 μm were 1.2, 12.7, and 37.2%, whereas at P28 the percentages were 6.1, 51.4, and 83.6%, respectively.

As an alternative method to demonstrate the increased threshold diameter required to initiate myelination in the dnβ1 mice, we compared the frequency distribution of the diameters of all myelinated and total axons (irrespective of myelination status) between wild-type and dnβ1 mutants in P17 optic nerve (Fig. 5 e). As predicted from the observations above, both the mean myelinated and unmyelinated axon diameters were significantly larger (P < 0.0001) in mutant optic nerves (0.86 ± 0.015 μm for myelinated axons, 0.38 ± 0.004 μm for unmyelinated axons) than in their wild-type littermate controls (0.75 ± 0.012 μm and 0.35 ± 0.004 μm, respectively). By contrast, the mean diameter of all axons was not significantly different, with an average axon diameter of 0.47 ± 0.006 μm and 0.48 ± 0.007 μm for wild-type and mutant, respectively (P = 0.21). This excludes the possibility that changes in the distribution of axon diameters might contribute to the effects on myelination we observe.

A greater threshold for myelination is also seen in FAK-deficient mice

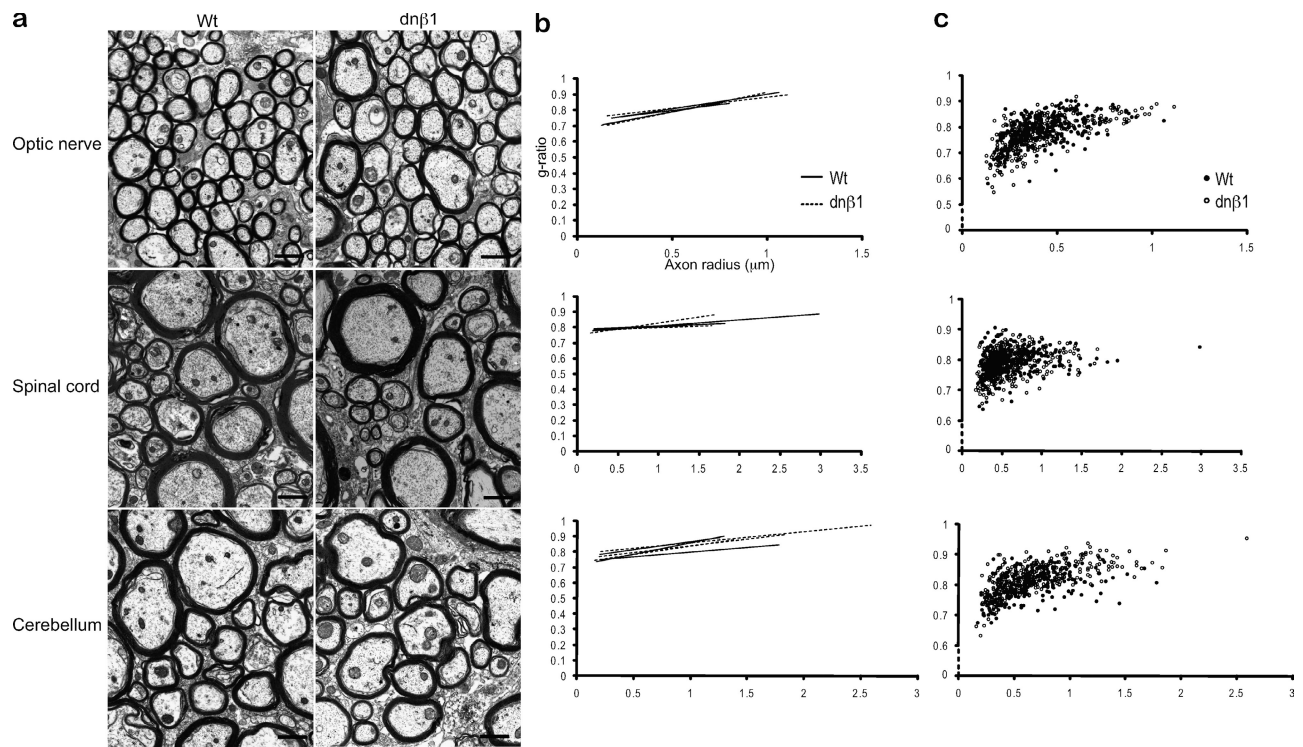If the increased threshold for myelination we observed in the dnβ1 mice reflects an inhibition of integrin signaling, then we

Figure 4. **The relationship between axon diameter and myelin thickness is normal in dnβ1 mice.** (a) Representative electron micrographs of sections of optic nerve, spinal cord, and cerebellum of P28 wild-type and dnβ1 mutant mice. Bar: 1 μm. (b) The linear regression of the g-ratio measurements for each animal ($n = 3$) is shown for the three CNS areas. Solid and dashed lines represent wild-type and mutant animals, respectively. (c) Scatter plot displays g-ratios of individual myelinated axons (obtained from three animals) as a function of the respective axon size. Closed and open circles represent wild-type and mutant axons, respectively.

would predict that other transgenic mice having perturbations of downstream signaling molecules should show a similar phenotype. To test this we examined P16–P21 optic nerves from mice in which FAK had been deleted in myelinating glial cells by crossing mice homozygous for a floxed FAK allele with a Cnp-Cre line (Grove et al., 2007). As discussed above, FAK is a key part of the integrin signaling pathway, binding to the integrin cytoplasmic domain and being activated by phosphorylation after integrin ligand binding, and loss of FAK activity in oligodendrocytes has very recently been shown to result in hypomyelination in the developing mouse optic nerve (Forrest et al., 2009). Similarly to the dnβ1 mice, we found that an increased threshold diameter was required for myelination at this age, as evidenced by a reduced percentage of myelinated axons in knockout (57.37 ± 10.38%, $n = 2,186$ from 4 animals) compared with wild-type (64.93 ± 10.70%, $n = 2,560$ from 4 animals) optic nerves of P16–P21 animals (P = 0.0087; Fig. 6), whereas there was no difference in the percentage of myelinated axons in adult (P60) nerves (Fig. S3).

Dnβ1 oligodendrocytes myelinate a reduced number of internodes in myelinating co-cultures

There are two general mechanisms by which the increase in axon diameter required for myelination in the P17 optic nerve might be explained. First, an intrinsic abnormality of the oligodendrocyte such that it cannot respond appropriately to the axoglial signal proportional to axon diameter that is required to

initiate myelination. As a result, the smallest axons no longer generate a signal within the oligodendrocyte of sufficient strength to trigger myelination. Second, a reduction in oligodendrocyte numbers such that there are no longer sufficient cells to myelinate all available axons. In this last situation, it would be expected that those axons myelinated last during development, i.e., the smallest-diameter axons (Remahl and Hildebrand, 1982), would be myelinated late or not at all during development in the mutant mouse. The former mechanism represents an intrinsic defect in the oligodendrocyte, whereas the latter is an extrinsic effect secondary to a reduction in cell numbers.

To discern which mechanism is responsible for our observations, we performed co-culture experiments in which oligodendrocytes are provided in considerable excess (thus eliminating any extrinsic effects of cell number variation) and examined myelination by oligodendrocytes derived from wild-type or dnβ1 mice. These oligodendrocytes were cultured in the presence of wild-type dorsal root ganglion (DRG) neurons and their myelination efficiency was evaluated as described elsewhere (Wang et al., 2007) by determining the percentage of oligodendrocytes forming myelin. Although not the normal target of CNS oligodendrocytes, axons formed by DRG neurones grown in culture have a range of diameters of less than 2 μm (Fig. S4 a), similar to those in the optic nerve studied here, and are myelinated by oligodendrocytes added to these cultures. They therefore provide an appropriate test of the intrinsic myelinogenic capacity of the oligodendrocyte. We found that dnβ1 oligodendrocytes myelinated DRG axons significantly less efficiently
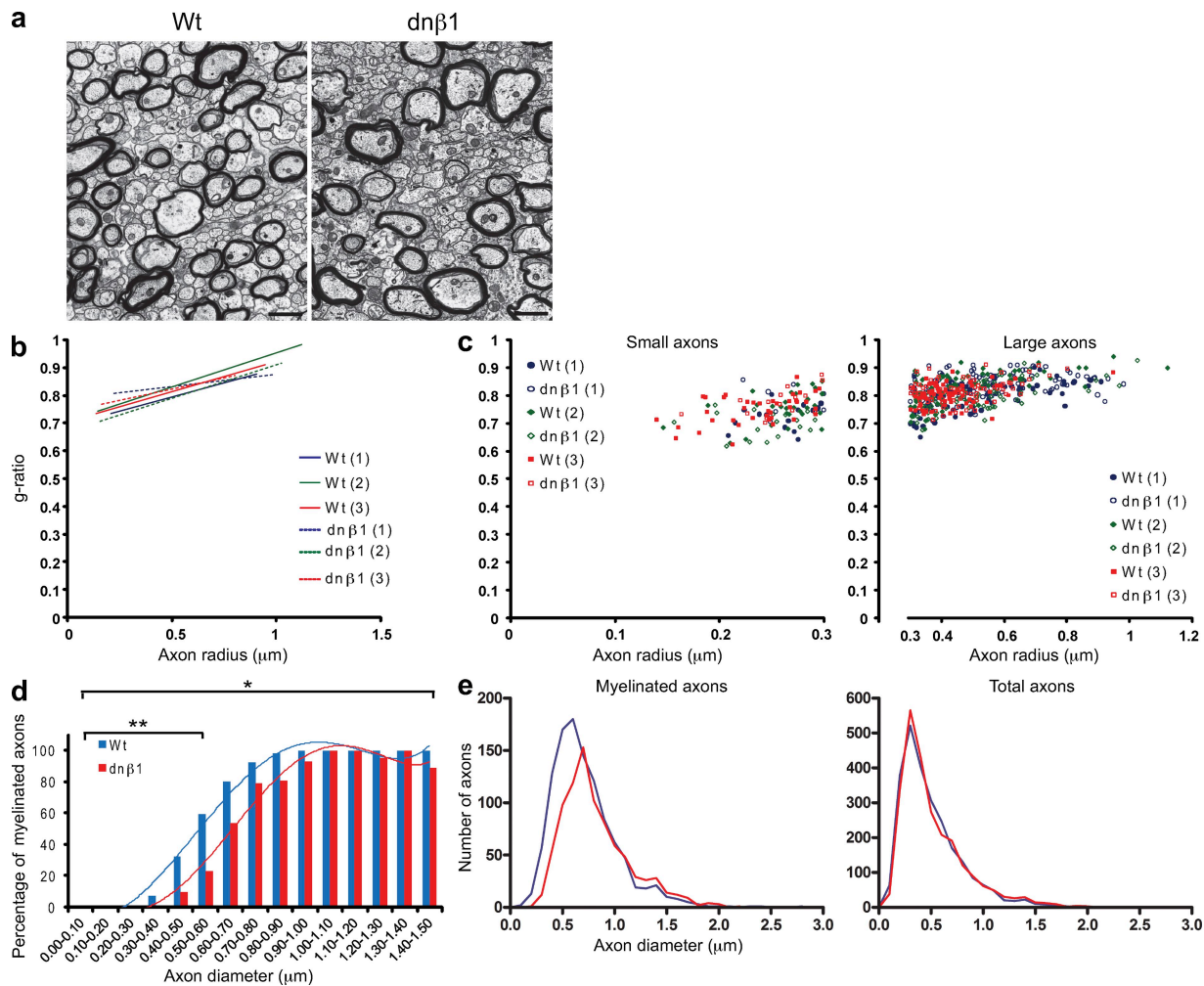
Figure 5. **The axon diameter required to initiate myelination is increased in the dnβ1 mice.** (a) Representative electron micrographs show a reduction in the frequency of small myelinated axons in optic nerve sections of P17 dnβ1 mutant mice compared with wild-type mice. Bar: 1 μm. (b) Normal myelin morphology and thickness in P17 optic nerve of dnβ1 mice. The linear regression of the g-ratio measurements for each animal (*n* = 3) is shown. Solid and dashed lines represent wild-type and mutant animals, respectively, from three litters displayed in blue, green, and red. (c) A reduced number of myelinated small-diameter axons is observed in dnβ1 mutants (open figures) compared with wild-type animals (closed figures). This is especially clear in two of the three litters analyzed, identified by different colors as in b. The scatter plots shown display g-ratios of individual myelinated axons as a function of the respective axon size, with the two parts of the plot corresponding to small and large axons shown separately (in left and right panels, respectively) and the former expanded to show the differences more clearly. Closed and open figures represent wild-type and mutant axons, respectively. (d) Representative graph from one litter shows the percentage of myelinated axons with respect to axon diameter at 0.1 μm intervals for wild-type and dnβ1 mice. A polynomial trendline was adjusted to the data. A reduced percentage of myelination across all axon diameter intervals is present in dnβ1 mutant compared with wild-type mice (*, P < 0.05), a phenotype most evident in small axons below 0.6 μm of diameter (**, P < 0.01). (e) Frequency histogram of the diameter of all the myelinated and total (both myelinated and unmyelinated) axons shows a shift of myelinated axons toward larger diameters in mutant animals, whereas the total distribution of axon diameters remains unchanged.

(P < 0.01) than wild-type oligodendrocytes (Fig. 7). To show any intrinsic defect more clearly, we then asked whether each dnβ1 oligodendrocyte myelinated a reduced number of internodes and/or internodes with reduced length. We therefore quantified for each individual cell the number and average length of internodes in a total of 50 wild-type and dnβ1 oligodendrocytes in co-culture. Dnβ1 oligodendrocytes showed a reduced number of internodes (37 ± 2) when compared with wild-type (50 ± 5) oligodendrocytes (P < 0.05, *n* = 5). This difference was not due either to a reduced neurite density or perturbed oligodendrocyte differentiation in the dnβ1 cultures, as these were similar in the cultures of all three genotypes (Fig. S4 b). By contrast, no difference was found between the average internodal length per oligodendrocyte from the two genotypes (Fig. S4 c,

wild-type: 45.8 ± 0.9 μm; dnβ1: 44.2 ± 0.8 μm, *n* = 5) or in the number of primary processes generated by each oligodendrocyte (wild-type: 4.12 ± 0.10, *n* = 74 from 4 experiments; dnβ1: 4.25 ± 0.12, *n* = 79 from 4 experiments). We conclude, therefore, that the increased axon diameter required for myelination reflects an intrinsic abnormality of axoglial signaling within the dnβ1 oligodendrocytes.

Dnβ3 mice show no evidence of altered axon diameter threshold for myelination

A concern with the use of the dominant-negative expression strategy is that the phenotype might reflect nonspecific effects of transgene expression on the cell surface. To control for this, we generated a second line of mice expressing a dominant-negative
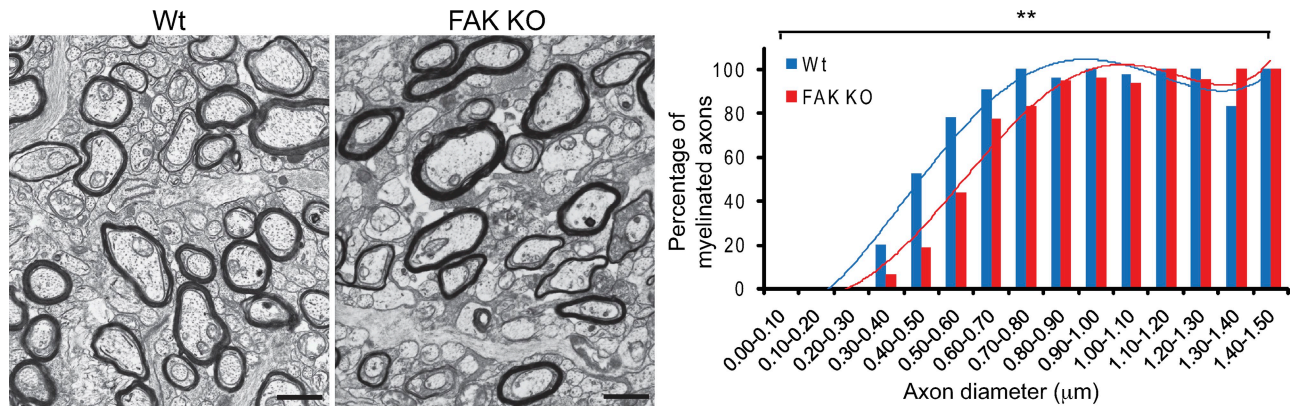
Figure 6. **A greater threshold for myelination is also seen in FAK-deficient mice.** (Left) Representative electron micrographs show a reduction in the frequency of small myelinated axons in optic nerve sections of P16-P21 FAK knockout mice compared with wild-type mice. Bar: 1 μm. (Right) Representative graph from one litter shows the percentage of myelinated axons with respect to axon diameter at 0.1-μm intervals for wild-type and dnβ1 mice. A polynomial trendline was adjusted to the data. A reduced percentage of myelination across all axon diameter intervals is present in FAK knockout compared with wild-type mice (**, P < 0.01).

subunit for β3 integrin (Fig. S5). β3 integrin is expressed on oligodendrocyte precursors but is not present at the myelinating stages (Milner et al., 1997). The construct used is identical to that for the dnβ1 mice except for the substitution of a β3 cytoplasmic domain for the β1 sequences. The same hprt targeting method was used to generate the dnβ3 transgenic mice, thus creating single-copy insertion into exactly the same locus as with the dnβ1 mice. This ensures comparable expression of the two coding sequences, as confirmed by immunofluorescence analysis showing the distribution and expression pattern of the dnβ3 protein to be the same as that previously seen for dnβ1 protein (Fig. S5). Hemizygous and wild-type male littermate mice were generated and compared with the dnβ1 mice. Dnβ3 mice revealed no defect in CNS myelination at P17 with no significant differences seen in the percentage of axons myelinated across all axonal intervals (dnβ3: 58.73 ± 10.54, n = 1,397 from 3 animals; wild type: 54.07 ± 10.41, n = 1,416 from 3 animals; P = 0.24) and no evidence for a lack of myelination in the smaller-diameter axons as seen for the dnβ1 mice (Fig. 8). Equally, no effect of the expression of dnβ3 on the myelination efficiency, the number of internodes, and the number of processes formed by each individual oligodendrocyte was detected in the myelinating co-culture assay. Dnβ3 oligodendrocytes generated 47 ± 1 internodes of average length 43.6 ± 0.6 μm and 4.44 ± 0.10 primary processes (n = 98 from 4 experiments), numbers not significantly different from wild-type cells (Fig. 7). We conclude that the phenotype we observed in the dnβ1 mice is not a nonspecific effect of transgene expression, but rather a specific effect of perturbing β1 integrin signaling.

Discussion

We show that oligodendrocytes expressing a single copy of a dominant-negative β1 integrin transgene myelinate small-diameter axons in optic nerve less efficiently than wild-type or control (dominant-negative β3) oligodendrocytes. This presents as a transient failure to myelinate small-diameter axons during development, demonstrated by a shift to the right of the dose–response

curve created by plotting axon diameter versus the percentage myelinated as schematized in Fig. 9. A similar phenotype was seen when the downstream signaling molecule FAK was deleted in myelinating glial cells. In mice expressing the dominant-negative β1 integrin transgene, we also observed that the thickness of the myelin sheath in those axons that do become myelinated is normal, as is the length of the myelin internodes as measured in myelinating co-cultures. We conclude, therefore, that inhibition of integrin signaling delays the initiation of myelination but has no effect on the signals required for the formation of the sheath once the axoglial interactions that lead to myelination have been established. It follows, therefore, that integrins contribute to the axoglial interactions that initiate myelination.

Given the evidence from myelinating co-culture experiments revealing an intrinsic defect in oligodendrocyte myelination, two broad mechanisms can be put forward to explain our observations—perturbation of the axoglial signaling that initiates myelination or a failure of oligodendrocyte differentiation (Fig. 10). The first would be based on the observation that in the PNS an axonal signal proportional to the diameter and above a certain threshold is required to initiate myelination by the contacting glial cell (Taveggia et al., 2005; Nave and Salzer, 2006). If there is a reduction in the glial response to the axonal signal due to perturbation of integrins, then the prediction would be that the signal on the small axons will not be detected as above the required level and a reduced percentage of myelination of these small-diameter axons will be observed. In contrast, the large axons could either provide a signal that is in excess of the threshold level or express an additional signaling molecule that initiates myelination without any requirement for integrin function, and thus would not be affected by integrin perturbation. In the second mechanism, small-diameter axons could be preferentially affected by the reduction in β1 integrin signaling as a result of a compromised ability of the oligodendrocyte to change their morphology and generate multiple processes for myelination. It has been shown that toad oligodendrocytes myelinating small axons extend more processes than those myelinating large axons (Stensaas and Stensaas, 1968; Hildebrand et al., 1993).
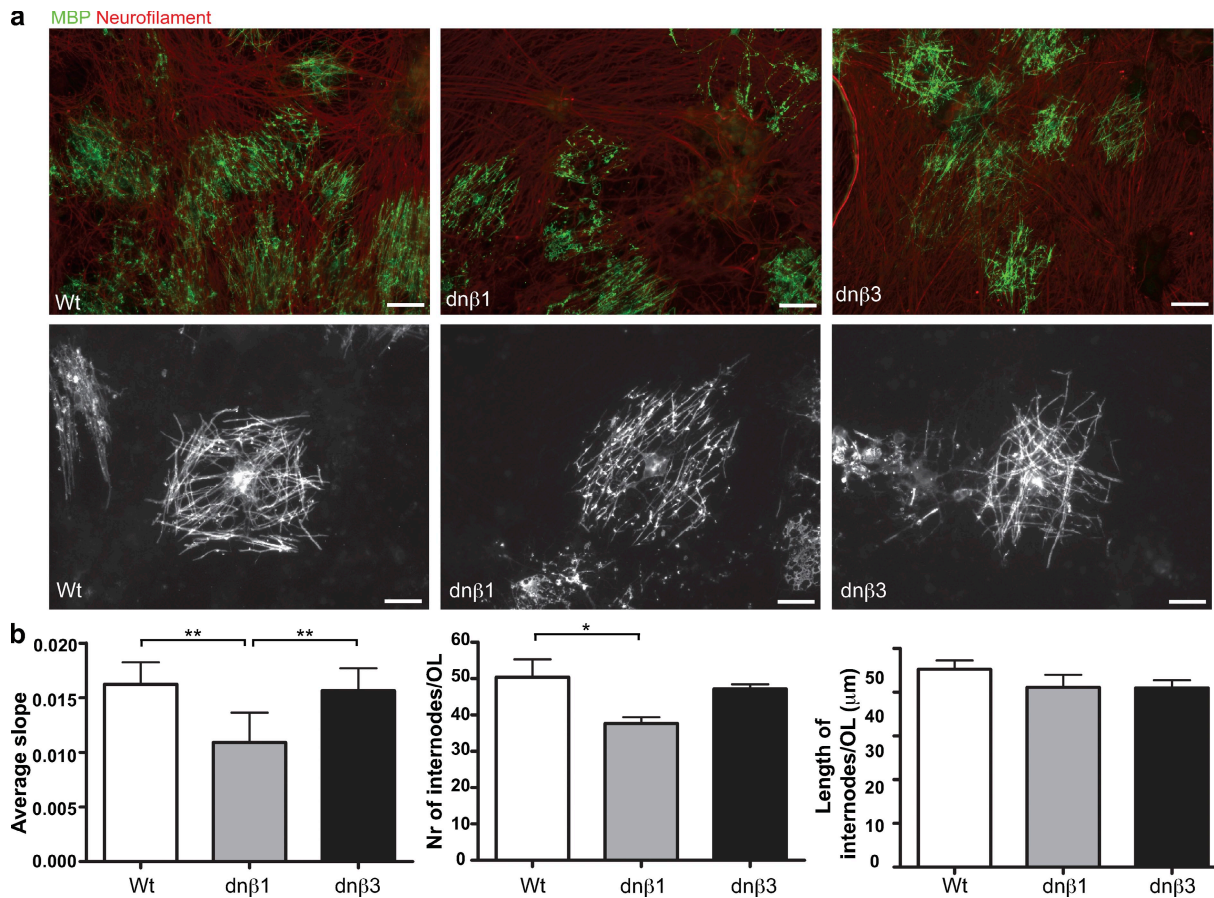
a MBP Neurofilament

b

Figure 7. Dnβ1 oligodendrocytes myelinate a reduced number of internodes in myelinating co-cultures. (a) Representative pictures are shown for wild-type, dnβ1, and dnβ3 MBP⁺ oligodendrocytes myelinating neurites within DRG neuron cultures at low (top panels) and high (bottom panels) magnification. Bars: top, 133 μm; bottom, 50 μm. (b) (left) Neurosphere-derived dnβ1 oligodendrocytes myelinate DRG neurons less efficiently than their wild-type or dnβ3 counterparts. Error bars represent SD (**, P < 0.01). The internodal number (middle) and length (right) were quantified for each oligodendrocyte (10 oligodendrocytes per experiment, n = 5). Dnβ1 oligodendrocytes showed a decrease in the internodal number per oligodendrocyte (*, P < 0.05), whereas the internodal length was unchanged for the three genotypes.

Additionally, oligodendrocytes in rat white matter areas constituted of small axons possess more branches than those in areas with both large and small axons (Matthews and Duncan, 1971). A reduction in β1 integrin signaling that compromises process outgrowth via the established role of this receptor in cytoskeletal reorganization would therefore be expected to reveal a phenotype in those tracts where more processes are required, i.e., those with small-diameter axons. In agreement with this, knockout mice for the regulator of the actin cytoskeleton WAVE1 exhibited a reduced number of myelinated axons in the optic nerve
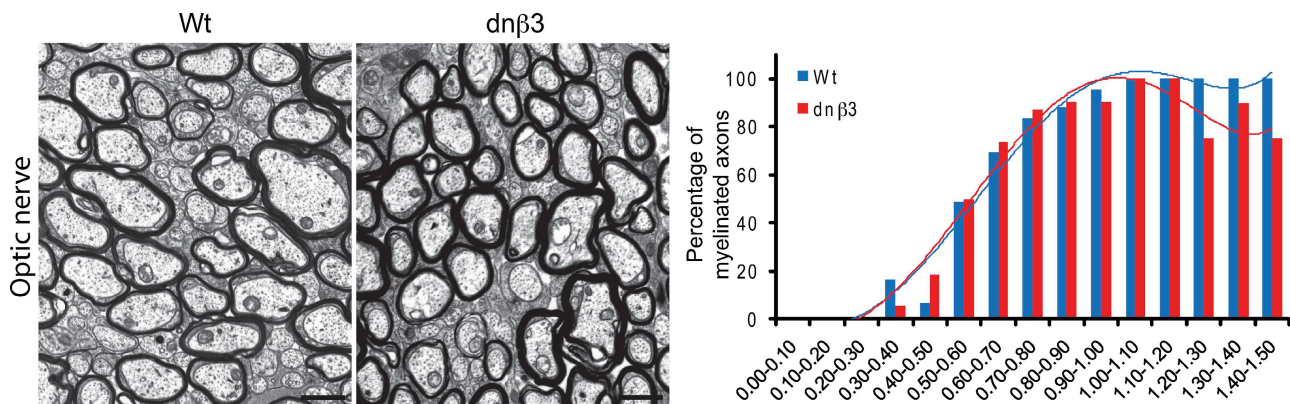

Figure 8. Dnβ3 mice show no evidence of altered axon diameter threshold for myelination. (Left) Representative electron micrographs of optic nerve sections of P17 wild-type and dnβ3 transgenic mice show no differences. Bar: 1 μm. (Right) Representative graph from one litter shows the percentage of myelinated axons with respect to axon diameter at 0.1-μm intervals for wild-type and dnβ3 mice. A polynomial trendline was adjusted to the data. The axon diameter threshold for myelination is unaffected in dnβ3 transgenic mice.

and corpus callosum, with WAVE1 knockout oligodendrocytes showing a reduced number of processes in cell culture (Kim et al., 2006).

Three observations argue against the latter mechanism—perturbation of cytoskeletal function as the cause of the phenotype in the dnβ1 mice. First, although the number of internodes myelinated by each dnβ1 oligodendrocyte in the myelinating cocultures is reduced, the length of internodes is unaltered, with the majority of internodes myelinated by wild-type, dnβ1, and dnβ3 oligodendrocytes distributed between 27 and 40 μm as recently reported for cortical oligodendrocytes in vivo (Murtie et al., 2007; Fig. S4 c). A compromised ability of the oligodendrocyte to extend processes would be expected both to reduce the number of internodes and to shorten internodal length, as this latter measurement must reflect process extension along the axon once contact has been established. Second, the similar g-ratios seen in the P17 optic nerve of wild-type and dnβ1 mice show that the cytoskeletal reorganization required for myelin sheath compaction is not affected by inhibition of integrin signaling. Third, the number of primary processes is not significantly different between wild-type, dnβ1, and dnβ3 oligodendrocytes in premyelinating co-cultures. Dnβ1 oligodendrocytes are, therefore, able to extend processes normally, as evidenced by their number of primary processes and internodal length, but then myelinate less efficiently with fewer internodes.

The conclusion that oligodendrocyte integrins form part of the recognition complex for axonal signals that determine whether or not myelination occurs is important, as the identity of such axonal signals in the CNS is unknown. In the PNS, the level of axonal type III Nrg1 has been shown to play a crucial role in determining both whether an axon is myelinated and in the regulation of myelin thickness (Michailov et al., 2004; Taveggia et al., 2005). We have shown that laminin-binding integrins amplify neuregulin signaling as part of the mechanisms that regulate target-dependent survival of newly formed oligodendrocytes in the CNS (Colognato et al., 2002). Our results here would therefore be consistent with a model in which axonal neuregulins in the CNS, recognized by oligodendrocyte ErbB receptors, generate a signal to initiate myelination that is further amplified by integrins. In the case of small-diameter axons, this amplification is essential for triggering myelination, whereas large-diameter axons generate sufficient signal without integrin amplification. However, the role of neuregulins in CNS myelination has not been resolved. Exogenous addition of Nrg1 promotes myelination in co-cultures of oligodendrocytes and DRG neurons (Wang et al., 2007) and myelination of type III Nrg1-deficient DRG neurons is significantly reduced in co-culture (Taveggia et al., 2008). Hypomyelination is seen in transgenic mice expressing a dominant-negative ErbB receptor in oligodendrocytes, and in mice haploinsufficient for type III Nrg1 (Roy et al., 2007; Taveggia et al., 2008). However, in contrast to the PNS, increased expression of this axonal signal does not promote myelination of very small, and normally unmyelinated, axons in co-cultures of superior cervical ganglion neurons and oligodendrocytes (Taveggia et al., 2008). Moreover, conditional mutants with ablation of Nrg1, ErbB3, or ErbB4 exhibit no cortical myelination abnormalities (Brinkmann et al., 2008),
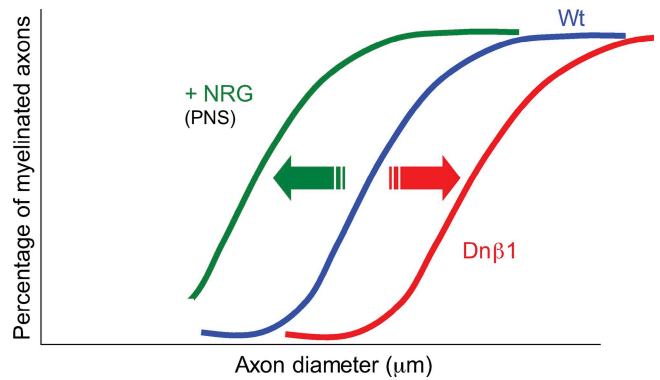

Figure 9. **The expression of dnβ1 integrin shifts the axon diameter threshold for myelination toward larger diameters, shown here schematically by a shift to the right of the dose–response curve created by plotting the percentage of axons myelinated against the axon diameter.** By contrast, the increased expression of Nrg1 in the PNS was previously shown to shift the myelination threshold toward lower axon sizes, i.e., to the left.

a result that rather compellingly argues against a necessary role for Nrg1 signaling in CNS myelination. Additional neuregulin isoforms may be important in the CNS but equally, and in contrast to the PNS, other axonal signals may be required for regulating myelination. These may also be amplified by integrins, as seen for a number of different growth factors in other cell types. The hypothesis that such multi-component signaling complexes initiate and regulate myelination by oligodendrocytes provides a mechanism to explain the "catch-up" by the mutant oligodendrocytes in the older animals, as compensatory interactions within the complex will facilitate restoration of normal axoglial interactions.

Interestingly, both in monkeys and humans the area of the CNS most prone to remyelination failure is the optic nerve (Lachapelle et al., 2005). A model in which amplification of a myelination signal is required for small- but not large-diameter axon myelination could explain both the vulnerability of the optic nerve and the regional selectivity of the phenotype seen in the dnβ1 mouse, as the optic nerve contains entirely small-diameter axons. Similar regional differences in myelination are observed in other mutants that perturb integrin signaling, such as the Fyn knockout and the laminin-2–deficient (dy/dy) mouse. In these mice myelination defects are seen in optic nerve but not in spinal cord, where the density of larger axons is higher. Another possibility to explain regional heterogeneity, intrinsic differences in the oligodendrocytes arising from different regions of the developing CNS, seems less likely given that ablation of one such population is followed by replacement from a different region (Kessaris et al., 2006). In addition, transplantation of oligodendrocytes from optic nerve into spinal cord reveals that the transplanted cells can myelinate the full range of axon diameters in their new environment, even though these diameters are much greater than those present in their original location (Fanarraga et al., 1998).

Although the two previous studies examining the role of β1 integrins in regulating CNS myelination appear contradictory (Benninger et al., 2006; Lee et al., 2006), the current study allows their reconciliation. Here we have concluded that inhibition of integrins perturbs axoglial signaling and delays myelination of
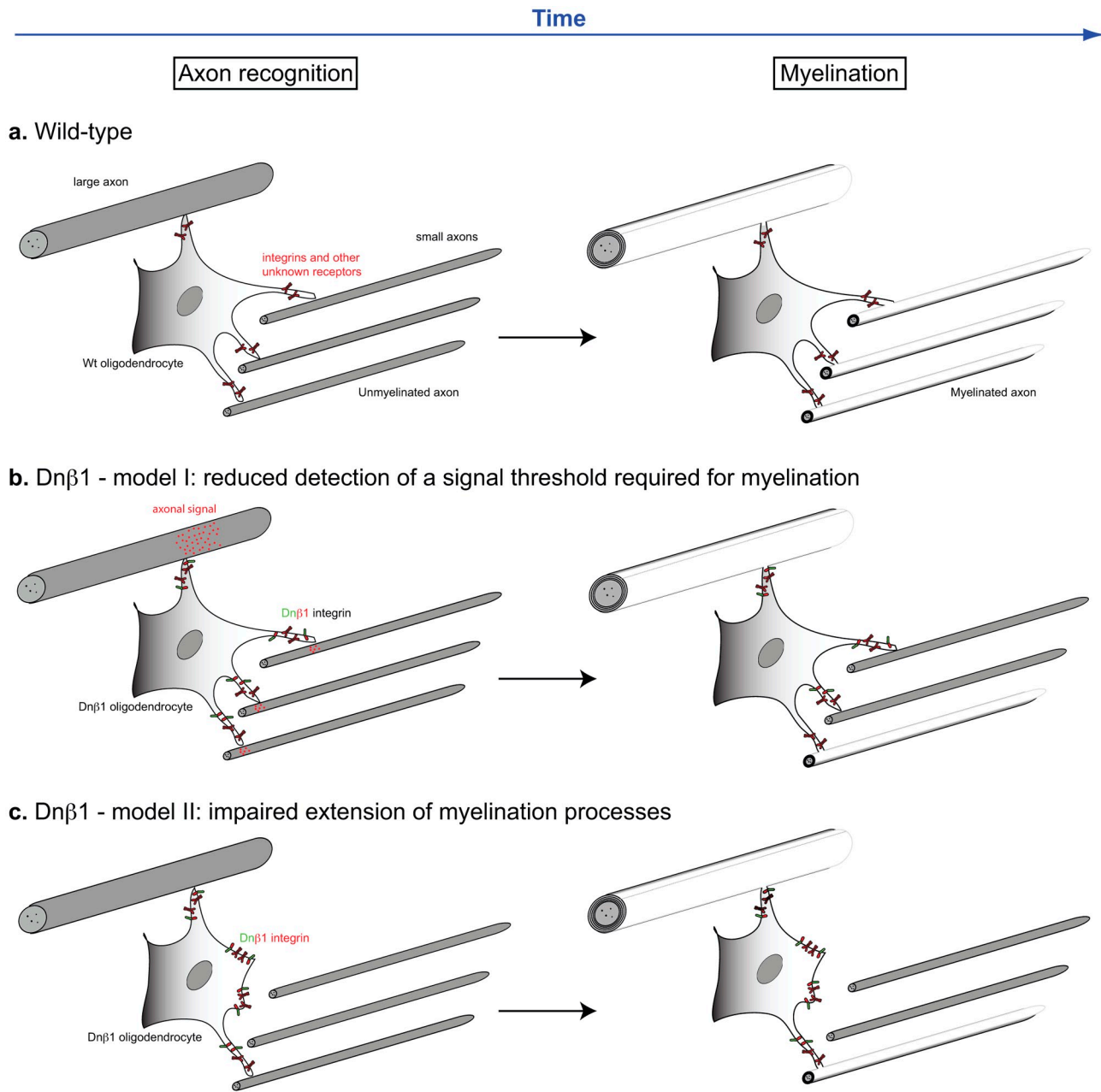
Time

Axon recognition

Myelination

a. Wild-type

large axon

small axons

integrins and other
unknown receptors

Wt oligodendrocyte

Unmyelinated axon

Myelinated axon

b. Dnβ1 - model I: reduced detection of a signal threshold required for myelination

axonal signal

Dnβ1 integrin

Dnβ1 oligodendrocyte

c. Dnβ1 - model II: impaired extension of myelination processes

Dnβ1 integrin

Dnβ1 oligodendrocyte

Figure 10. **Models for the failure in myelination of small-diameter axons resulting from perturbed β1 integrin signaling.** (a) The oligodendrocyte initially extends processes to reach large and small axons and then initiates myelination. Large axons are myelinated earlier than small axons. (b) Model I: an axonal signal proportional to the diameter and above a certain threshold is required to initiate myelination by the contacting glial cell. Due to the expression of dnβ1 integrin there is a reduction in the glial signaling in response to this signal, such that the signal initiated by some small axons will now not be above the required (threshold) level for myelination. By contrast, the large axons provide a signal that is significantly in excess of the threshold level and/or additional signals, and thus will not be affected by perturbation of integrin signaling. (c) Model II: myelinating tracts rich in small-diameter axons require more oligodendrocyte processes than those tracts rich in large axons. Small axons are, therefore, particularly susceptible to any failure of the oligodendrocyte to generate multiple processes for myelination, as might occur after perturbation of integrin signaling, leading to an impaired ability of the cell to reorganize the cytoskeleton. See text for a discussion of the evidence for and against the two models.

small-diameter axons, but has no effect on the subsequent formation of the myelin sheath. This conclusion is consistent with our previous report on the absence of g-ratio disturbances in the oligodendrocyte-specific conditional β1 knockout (Benninger et al., 2006), where the analysis focused on myelin sheath thickness in older animals. Hypomyelination after expression of β1ΔC (Lee et al., 2006) can be explained by a requirement for dystroglycan in sheath formation. As noted in the introduction, the β1ΔC integrin

extracellular domain will form heterodimers with integrin-α subunits and thus compete for ligand with other oligodendroglial laminin receptors. One of these is dystroglycan (Colognato et al., 2007), for which the main binding site on laminin overlaps with that of integrins at the laminin G domains LG1-3 (Talts et al., 1999; Wizemann et al., 2003). We have shown that dystroglycan is a significant laminin receptor for CNS myelination in vitro, and transgenic studies reveal an essential role in PNS

myelination (Saito et al., 2003; Occhi et al., 2005; Colognato et al., 2007). We propose, therefore, that the study of Lee et al. (2006) expressing β1ΔC reveals a requirement for dystroglycan in later stages of myelin sheath formation in addition to the role of integrins in the earlier stages of initiation. Our present and previous studies, by contrast, specifically target integrin signaling and would thus not reveal any later role of other laminin receptors.

The identification of the signals regulating the initiation of myelination may lead to the development of strategies to promote effective remyelination by oligodendrocytes within MS lesions arrested at the premyelinating stage and therefore unable to contribute to repair (Chang et al., 2002). Further studies examining the partners and ligands of the integrins expressed on oligodendrocytes represent promising new approaches toward understanding this goal.

Materials and methods

Cloning and dnβ1/dnβ3 ES cell generation
For the generation of the genetically modified embryonic stem (ES) cells expressing the dnβ1/dnβ3 integrin we used the hypoxanthine phosphoribosyl transferase (hprt) targeting system (Farhadi et al., 2003). This system relies on the use of an hprt-deficient ES cell line (Bronson et al., 1996; Farhadi et al., 2003) and on the cloning of the desired sequences onto a vector containing the deleted hprt sequences as well as the hprt homologous arms required for recombination.

The dominant-negative sequences were initially cloned into a Gateway entry vector containing the 9.5-Kb MBP promoter (pENTR1A9.5). The IL2Rβ1 integrin sequence was available (Relvas et al., 2001) cloned as an XhoI fragment into XhoI of pLXIN vector (Clontech Laboratories, Inc.). We subsequently subcloned IL2Rβ1 as an XhoIK-PstI + PstI-BamHI fragment into EcoRV-BamHI of pBluescript. The IL2Rβ1 was then excised as an XhoI-ClaI fragment from pBluescript and cloned into pENTR1A9.5 linearized with SalI-ClaI. The IL2Rβ3 integrin sequence was also available cloned as an XhoI fragment into XhoI of pLXIN vector (Clontech Laboratories, Inc.). We subsequently subcloned IL2Rβ3 as an XhoIK-HindIII + HindIII-BamHI fragment into EcoRV-BamHI of pBluescript. The IL2Rβ3 was then excised as an XhoI-ClaI fragment from pBluescript and cloned into pENTR1A9.5 linearized with SalI-ClaI. The clones were all confirmed by an extensive series of restriction digests and the final clones in pENTR1A9.5 were also confirmed by automatic sequencing using the primers pE9.5bS 5′-aaagcaggctttaaaggaacc-3′, pE9.5aC 5′-ggctgcaggaattcgatatca-3′, and pE9.5mbpF 5′-ttcccggggcatctcgggaaaag-3′, pE9.5mbpR 5′-aggccatcgcccctctggagtggt-3′. Transgenes cloned into pENTR1A9.5 vector were subsequently transferred to the hprt targeting destination vector, in vitro, using the Gateway technology (Invitrogen). Both transgenes were docked, in single copy and fixed orientation, in the 5′ flanking sequence of the hprt locus on the X chromosome. BPES5 ES cells (Denarier et al., 2005), bearing the same hprt deletion as the original BK4 ES cells (Bronson et al., 1996), were electroporated with 40 µg of linearized DNA and selected on HAT-supplemented medium as described previously (Farhadi et al., 2003). The HAT⁺ ES cell clones were screened by PCR using the primers ESIL2Rb1II 5′-cagagcttgtgcattgacattg-3′ and pE9.5aC.

Generation of dominant-negative β1/β3 integrin transgenic mice
The genetically altered agouti ES cells were subsequently injected into C57BL/6-derived blastocysts that were then transplanted into the uteri of recipient females. Resulting chimeric males were bred with C57BL/6 females, and the F1 female agouti offspring were backcrossed with C57BL/6 males. Genotyping was performed by PCR with a set of primers for the wild-type (PfHprt mus 5′-gagggagaaaaatgcggagtg-3′ and PrHprt mus 5′-ctccggaaagcagtgaggtaag-3′) and a set of primers for the transgenic (ESIL2Rb1II and pE9.5aC) alleles. When further confirmation of sex determination was required, especially at young ages, PCR for the sex-determining region Y (SRY) gene was additionally performed. Mutant homozygous females and hemizygous males of the two dominant-negative lines were viable and showed no obvious behavioral abnormalities.

FAK knockout mice
The conditional inactivation of FAK in myelinating cells by crossing transgenic mice with lox sites inserted into the FAK gene (McLean et al., 2004;

Charlesworth et al., 2006) with transgenic mice expressing cre recombinase under the regulation of the CNP promoter (a gift of Dr Klaus Nave, Gottingen, Germany) has been described elsewhere (Grove et al., 2007).

Myelinating co-cultures
Dorsal root ganglia (DRGs) were dissected from E14–E16 rats and digested for 45 min at 37°C with 1.2 U/ml papain (Worthington), 0.24 mg/ml L-cysteine (Sigma-Aldrich), and 40 µg/ml Dnase I (Sigma-Aldrich). The dissociated cells were plated onto 22-mm coverslips precoated with poly-D-lysine (10 µg/ml; Sigma-Aldrich) followed by matrigel (1:20 dilution; BD Biosciences) at a density of 5 × 10⁵ cells/ml. The DRGs were grown for two weeks in DMEM supplemented with 10% fetal bovine serum (Invitrogen) and nerve growth factor (NGF, 100 ηg/ml; AbD Serotec). The cultures were pulsed three times, for 2 d each time, with fluorodeoxyuridine (10 µM; Sigma-Aldrich) to remove contaminating fibroblasts and glial cells. Neurospheres from wild-type or mutant litters were added to each coverslip with purified DRGs. The medium used for the co-cultures was 50:50 DMEM/Neurobasal medium (Invitrogen) supplemented with Sato and B27 (Invitrogen), NGF (100 ηg/ml), N-acetyl cysteine (5 µg/ml, Sigma-Aldrich), and D-biotin (10 ηg/ml). Co-cultures were maintained for 3 wk with medium and supplements changed every 3–4 d. After 3 wk, the extent of myelination was quantified by determining the slope of the best-fit line defining the relationship between the percentage of oligodendrocytes (defined by the expression of MBP as detected by immunohistochemistry) with myelin sheaths and the density of the underlying neurite network (Wang et al., 2007). The number and length of internodes was traced and measured using ImageJ software. The average number of primary processes (defined as those originated directly from the cell body) was quantified in MBP⁺ oligodendrocytes at the initial stages of myelination, before internode formation, using OpenLab image analysis software (Improvision).

RT-PCR
Total RNA was extracted from mouse tissues using the RNeasy mini kit (QIAGEN), according to the manufacturer's instructions, and subjected to one-step RT-PCR (QIAGEN). The following primers were used for the extracellular β1 integrin domain: B1ecF 5′-tggacaatgtcacctggaaa-3′, B1ecR 5′-tgtgcccact-gctgacttag-3′; and for the IL2Rα extracellular domain: IL2RaF 5′-atcagtgcgtc-cagggatac-3′, IL2RaR 5′-gacgaggcaggaagtctcac-3′. Data were normalized to β-actin levels (5′-agccatgtacgtatccatcc-3′ and 5′-ctctcagctgtggtggtgaa-3′). ImageJ software was used to quantify mRNA expression levels.

Western blot
Dissected tissues from dnβ1 and wild-type mice were homogenized in 1% SDS and subjected to SDS-PAGE using appropriate percentage of acrylamide minigels. They were then transferred onto 0.45-µm nitrocellulose membranes (HybondC; GE Healthcare) and blocked with 5% nonfat dry milk and 0.1% Tween 20 Tris-buffered saline (TBS) for 1 h at room temperature (RT). The primary antibody diluted in blocking solution was incubated for 2 h at RT or overnight (ON) at 4°C. The blots were then washed three times in TBS 0.1% Tween (TBS-T) and incubated for 1 h at RT with a horseradish peroxidase–labeled secondary antibody (GE Healthcare). After washing again in TBS-T the immunoreactive proteins were revealed by chemiluminescence (ECL; GE Healthcare) according to the manufacturer's instructions. Digitalized images were obtained and bands quantified using ImageJ software.

Immunofluorescence and image acquisition
When staining for MBP on tissue sections, a post-fixation step prior staining was performed with 95% ethanol and 5% acetic acid for 30 min at −20°C, followed by three rinses in PBS. Sections were then blocked for 1 h in PBS containing 10% normal goat serum (NGS) and 0.1% Triton X-100 at RT, after which the primary antibody incubation was performed either ON at 4°C or for 2 h at RT. The following primary antibodies were used for immunofluorescence or Western blot: rat anti-MBP (AbD Serotec), mouse anti-neurofilament 200 (Sigma-Aldrich), rabbit polyclonal anti-pFAK (Y397; Invitrogen), rabbit polyclonal anti-FAK (Invitrogen), and monoclonal mouse anti–human CD25/interleukin-2 α receptor (Dako). After washing in PBS, the sections were incubated for 1 h with the secondary antibody (FITC or Alexa 588 and TRITC or Alexa 488 labeled) and Hoechst. After further washes in PBS, slides were mounted in fluoromount (SouthernBiotech). All fluorescence images were acquired at RT with a fluorescence microscope (Axioplan; Carl Zeiss, Inc.), fitted with 10x eyepiece magnification, 20x (0.5 NA) and 40x (0.75 NA) objectives, and a digital camera (model C4742-95; Hamamatsu) using OpenLab image analysis software (Improvision).

Electron microscopy

Hemizygous and wild-type males were used as mutant and control mice, respectively. Anaesthetized mice were perfused intracardially with freshly prepared 4% glutaraldehyde containing 2 mmol/l $CaCl_2$ in 0.1 M phosphate buffer (PB) at RT. Dissected tissues were incubated in the same solution ON. After rinsing in 0.1 M PB, samples were post-fixed in 1% osmium tetroxide ON and dehydrated in a grade series of ethanol. The tissues were embedded in TAAB resin, and sections for light and electron microscopy were prepared using a microtome (Ultracut UCT; Leica). Semi-thin sections were stained with methylene blue. Ultra-thin sections were stained with saturated uranyl acetate in 50% ethanol and lead citrate and examined in a transmission electron microscope (model CM100; Philips).

Morphometry

Digitalized images were obtained from corresponding levels of the various mouse tissues. The g-ratio was calculated by the ratio between the area of the axon and the area of the same axon including myelin using OpenLab image analysis software (Improvision). A minimum of 100 randomly chosen axons, from at least 5 nonoverlapping images per animal, were analyzed for calculating the g-ratio. A minimum of 400 axons from at least 3 nonoverlapping images per animal were analyzed to calculate the percentage of myelination per axon diameter.

Statistical analysis

The data show the mean ± SEM, unless otherwise indicated. Statistical significance for the expression of the dnβ1 integrin by RT-PCR and changes in pFAK by Western blot was determined by using paired *t* test; for g-ratio analysis by Student's *t* test; for percentage of myelination per axon diameter analysis by two-way ANOVA; for average axon diameter determination by Student's *t* test; for evaluation of myelination efficiency in co-culture by repeated measures ANOVA with Tukey's multiple comparison post-test; and for internodal number, internodal length, and number of processes analyses by one-way ANOVA with Tukey's multiple comparison post-test. *n* represents the number of axons examined for each control and mutant littermate, with at least three independent litters of transgenic mice analyzed unless otherwise indicated or, in the case of the co-cultures, the number of independent experiments performed. Statistical analysis was performed using GraphPad Prism software.

Online supplemental material

Figure S1 shows the expression pattern in the brain and optic nerve of the 9.5-Kb MBP promoter used for the dominant-negative integrins. This promoter is expressed only at the time of myelination in different white matter tracts. Figure S2 shows that the morphology of corpus callosum and optic nerve in the dnβ1 mice is normal, as assessed by immunohistochemistry. Figure S3 shows that the threshold axon diameter for myelination is normal in adult dnβ1 and FAK KO mice. Figure S4 provides further quantification of the myelinating co-cultures, showing the distribution of axon diameters and that oligodendrocyte differentiation and internodal length are similar in cultures using cells from wt, dnβ1, and dnβ3 mice. Figure S5 illustrates the steps taken to generate and characterize the dnβ3 transgenic line used as a control in our study. Online supplemental material is available at http://www.jcb.org/cgi/content/full/jcb.200807010/DC1.

References

Benninger, Y., H. Colognato, T. Thurnherr, R.J. Franklin, D.P. Leone, S. Atanasoski, K.A. Nave, C. ffrench-Constant, U. Suter, and J.B. Relvas. 2006. Beta1-integrin signaling mediates premyelinating oligodendrocyte survival but is not required for CNS myelination and remyelination. *J. Neurosci.* 26:7665–7673.

Brinkmann, B.G., A. Agarwal, M.W. Sereda, A.N. Garratt, T. Müller, H. Wende, R.M. Stassart, S. Nawaz, C. Humml, V. Velanac, et al. 2008. Neuregulin-1/ErbB signaling serves distinct functions in myelination of the peripheral and central nervous system. *Neuron.* 59:581–595.

Bronson, S.K., E.G. Plaehn, K.D. Kluckman, J.R. Hagaman, N. Maeda, and O. Smithies. 1996. Single-copy transgenic mice with chosen-site integration. *Proc. Natl. Acad. Sci. USA.* 93:9067–9072.

Cahoy, J.D., B. Emery, A. Kaushal, L.C. Foo, J.L. Zamanian, K.S. Christopherson, Y. Xing, J.L. Lubischer, P.A. Krieg, S.A. Krupenko, et al. 2008. A transcriptome database for astrocytes, neurons, and oligodendrocytes: a new resource for understanding brain development and function. *J. Neurosci.* 28:264–278.

Chang, A., W.W. Tourtellotte, R. Rudick, and B.D. Trapp. 2002. Premyelinating oligodendrocytes in chronic lesions of multiple sclerosis. *N. Engl. J. Med.* 346:165–173.

Charlesworth, P., N.H. Komiyama, and S.G. Grant. 2006. Homozygous mutation of focal adhesion kinase in embryonic stem cell derived neurons: normal electrophysiological and morphological properties in vitro. *BMC Neurosci.* 7:47.

Colognato, H., W. Baron, V. Avellana-Adalid, J.B. Relvas, A. Baron-Van Evercooren, E. Georges-Labouesse, and C. ffrench-Constant. 2002. CNS integrins switch growth factor signalling to promote target-dependent survival. *Nat. Cell Biol.* 4:833–841.

Colognato, H., J. Galvin, Z. Wang, J. Relucio, T. Nguyen, D. Harrison, P.D. Yurchenco, and C. ffrench-Constant. 2007. Identification of dystroglycan as a second laminin receptor in oligodendrocytes, with a role in myelination. *Development.* 134:1723–1736.

Denarier, E., R. Forghani, H.F. Farhadi, S. Dib, N. Dionne, H.C. Friedman, P. Lepage, T.J. Hudson, R. Drouin, and A. Peterson. 2005. Functional organization of a Schwann cell enhancer. *J. Neurosci.* 25:11210–11217.

Fanarraga, M.L., I.R. Griffiths, M. Zhao, and I.D. Duncan. 1998. Oligodendrocytes are not inherently programmed to myelinate a specific size of axon. *J. Comp. Neurol.* 399:94–100.

Farhadi, H.F., P. Lepage, R. Forghani, H.C. Friedman, W. Orfali, L. Jasmin, W. Miller, T.J. Hudson, and A.C. Peterson. 2003. A combinatorial network of evolutionarily conserved myelin basic protein regulatory sequences confers distinct glial-specific phenotypes. *J. Neurosci.* 23:10214–10223.

Fassler, R., and M. Meyer. 1995. Consequences of lack of beta 1 integrin gene expression in mice. *Genes Dev.* 9:1896–1908.

Forrest, A.D., H.E. Beggs, L.F. Reichardt, J.L. Dupree, R.J. Colello, and B. Fuss. 2009. Focal adhesion kinase (FAK): a regulator of CNS myelination. *J. Neurosci. Res.* epub ahead of print.

Friede, R.L. 1972. Control of myelin formation by axon caliber (with a model of the control mechanism). *J. Comp. Neurol.* 144:233–252.

Grove, M., N.H. Komiyama, K.A. Nave, S.G. Grant, D.L. Sherman, and P.J. Brophy. 2007. FAK is required for axonal sorting by Schwann cells. *J. Cell Biol.* 176:277–282.

Hildebrand, C., S. Remahl, H. Persson, and C. Bjartmar. 1993. Myelinated nerve fibres in the CNS. *Prog. Neurobiol.* 40:319–384.

Kessaris, N., M. Fogarty, P. Iannarelli, M. Grist, M. Wegner, and W.D. Richardson. 2006. Competing waves of oligodendrocytes in the forebrain and postnatal elimination of an embryonic lineage. *Nat. Neurosci.* 9:173–179.

Kim, H.J., A.B. DiBernardo, J.A. Sloane, M.N. Rasband, D. Solomon, B. Kosaras, S.P. Kwak, and T.K. Vartanian. 2006. WAVE1 is required for oligodendrocyte morphogenesis and normal CNS myelination. *J. Neurosci.* 26:5849–5859.

Lachapelle, F., C. Bachelin, P. Moissonnier, B. Nait-Oumesmar, A. Hidalgo, D. Fontaine, and A. Baron-Van Evercooren. 2005. Failure of remyelination in the nonhuman primate optic nerve. *Brain Pathol.* 15:198–207.

LaFlamme, S.E., L.A. Thomas, S.S. Yamada, and K.M. Yamada. 1994. Single subunit chimeric integrins as mimics and inhibitors of endogenous integrin functions in receptor localization, cell spreading and migration, and matrix assembly. *J. Cell Biol.* 126:1287–1298.

Laursen, L.S., and C. ffrench-Constant. 2007. Adhesion molecules in the regulation of CNS myelination. *Neuron Glia Biol.* 3:367–375.

Lee, K.K., Y. de Repentigny, R. Saulnier, P. Rippstein, W.B. Macklin, and R. Kothary. 2006. Dominant-negative beta1 integrin mice have region-specific myelin defects accompanied by alterations in MAPK activity. *Glia.* 53:836–844.

Martin-Bermudo, M.D., I. Alvarez-Garcia, and N.H. Brown. 1999. Migration of the *Drosophila* primordial midgut cells requires coordination of diverse PS integrin functions. *Development.* 126:5161–5169.

Matthews, M.A., and D. Duncan. 1971. A quantitative study of morphological changes accompanying the initiation and progress of myelin production in the dorsal funiculus of the rat spinal cord. *J. Comp. Neurol.* 142:1–22.

McLean, G.W., N.H. Komiyama, B. Serrels, H. Asano, L. Reynolds, F. Conti, K. Hodivala-Dilke, D. Metzger, P. Chambon, S.G. Grant, and M.C. Frame. 2004. Specific deletion of focal adhesion kinase suppresses tumor formation and blocks malignant progression. *Genes Dev.* 18:2998–3003.

Michailov, G.V., M.W. Sereda, B.G. Brinkmann, T.M. Fischer, B. Haug, C. Birchmeier, L. Role, C. Lai, M.H. Schwab, and K.A. Nave. 2004. Axonal neuregulin-1 regulates myelin sheath thickness. *Science.* 304:700–703.

Milner, R., E. Frost, S. Nishimura, M. Delcommenne, C. Streuli, R. Pytela, and C. ffrench-Constant. 1997. Expression of alpha vbeta3 and alpha vbeta8 integrins during oligodendrocyte precursor differentiation in the presence and absence of axons. *Glia.* 21:350–360.

Murtie, J.C., W.B. Macklin, and G. Corfas. 2007. Morphometric analysis of oligodendrocytes in the adult mouse frontal cortex. *J. Neurosci. Res.* 85:2080–2086.

Nave, K.A., and J.L. Salzer. 2006. Axonal regulation of myelination by neuregulin 1. *Curr. Opin. Neurobiol.* 16:492–500.

Occhi, S., D. Zambroni, U. Del Carro, S. Amadio, E.E. Sirkowski, S.S. Scherer, K.P. Campbell, S.A. Moore, Z.L. Chen, S. Strickland, et al. 2005. Both laminin and Schwann cell dystroglycan are necessary for proper clustering of sodium channels at nodes of Ranvier. *J. Neurosci.* 25:9418–9427.

Relvas, J.B., A. Setzu, W. Baron, P.C. Buttery, S.E. LaFlamme, R.J. Franklin, and C. ffrench-Constant. 2001. Expression of dominant-negative and chimeric subunits reveals an essential role for beta1 integrin during myelination. *Curr. Biol.* 11:1039–1043.

Remahl, S., and C. Hildebrand. 1982. Changing relation between onset of myelination and axon diameter range in developing feline white matter. *J. Neurol. Sci.* 54:33–45.

Roy, K., J.C. Murtie, B.F. El-Khodor, N. Edgar, S.P. Sardi, B.M. Hooks, M. Benoit-Marand, C. Chen, H. Moore, P. O'Donnell, et al. 2007. Loss of erbB signaling in oligodendrocytes alters myelin and dopaminergic function, a potential mechanism for neuropsychiatric disorders. *Proc. Natl. Acad. Sci. USA.* 104:8131–8136.

Saito, F., S.A. Moore, R. Barresi, M.D. Henry, A. Messing, S.E. Ross-Barta, R.D. Cohn, R.A. Williamson, K.A. Sluka, D.L. Sherman, et al. 2003. Unique role of dystroglycan in peripheral nerve myelination, nodal structure, and sodium channel stabilization. *Neuron.* 38:747–758.

Schaller, M.D., J.D. Hildebrand, J.D. Shannon, J.W. Fox, R.R. Vines, and J.T. Parsons. 1994. Autophosphorylation of the focal adhesion kinase, pp125FAK, directs SH2-dependent binding of pp60src. *Mol. Cell. Biol.* 14:1680–1688.

Stensaas, L.J., and S.S. Stensaas. 1968. Astrocytic neuroglial cells, oligodendrocytes and microgliacytes in the spinal cord of the toad. II. Electron microscopy. *Z. Zellforsch. Mikrosk. Anat.* 86:184–213.

Stephens, L.E., A.E. Sutherland, I.V. Klimanskaya, A. Andrieux, J. Meneses, R.A. Pedersen, and C.H. Damsky. 1995. Deletion of beta 1 integrins in mice results in inner cell mass failure and peri-implantation lethality. *Genes Dev.* 9:1883–1895.

Talts, J.F., Z. Andac, W. Gohring, A. Brancaccio, and R. Timpl. 1999. Binding of the G domains of laminin alpha1 and alpha2 chains and perlecan to heparin, sulfatides, alpha-dystroglycan and several extracellular matrix proteins. *EMBO J.* 18:863–870.

Taveggia, C., G. Zanazzi, A. Petrylak, H. Yano, J. Rosenbluth, S. Einheber, X. Xu, R.M. Esper, J.A. Loeb, P. Shrager, et al. 2005. Neuregulin-1 type III determines the ensheathment fate of axons. *Neuron.* 47:681–694.

Taveggia, C., P. Thaker, A. Petrylak, G.L. Caporaso, A. Toews, D.L. Falls, S. Einheber, and J.L. Salzer. 2008. Type III neuregulin-1 promotes oligodendrocyte myelination. *Glia.* 56:284–293.

Voyvodic, J.T. 1989. Target size regulates calibre and myelination of sympathetic axons. *Nature.* 342:430–433.

Wang, Z., H. Colognato, and C. ffrench-Constant. 2007. Contrasting effects of mitogenic growth factors on myelination in neuron-oligodendrocyte co-cultures. *Glia.* 55:537–545.

Waxman, S.G., and M.V. Bennett. 1972. Relative conduction velocities of small myelinated and non-myelinated fibres in the central nervous system. *Nat. New Biol.* 238:217–219.

Wizemann, H., J.H. Garbe, M.V. Friedrich, R. Timpl, T. Sasaki, and E. Hohenester. 2003. Distinct requirements for heparin and alpha-dystroglycan binding revealed by structure-based mutagenesis of the laminin alpha2 LG4-LG5 domain pair. *J. Mol. Biol.* 332:635–642.